PAPER • **OPEN ACCESS**

Experimental investigation of hydrodynamics and heat transfer of sphere cooling using air/water mist two phase flow

To cite this article: A H Abed *et al* 2019 *IOP Conf. Ser.: Mater. Sci. Eng.* **552** 012001

Experimental investigation of hydrodynamics and heat transfer of sphere cooling using air/water mist two phase flow

A H Abed[1, 2], S E Shcheklein[1], V M Pakhaluev[1]

[1]Department of Nuclear Power Plants and Renewable Energy Sources, Ural Federal University named after the first President of Russia B. N. Yeltsin, Mira St., 19, Yekaterinburg 620002, Russia
[2]Department of Electromechanical Engineering, University of Technology, Al-Sina'a Street, Baghdad 10066, Iraq

E-mail: akraaam82@yahoo.com

Abstract. To improve the cooling performance for the future generation of gas-cooled equipment, experimental studies on air/water mist heat transfer of single sphere inside a cylindrical channel have been carried out with an aim to investigate the heat transfer enhancement by suspending tiny water mist into air flow. The effect of the different key factors such the inlet Reynolds number, surface heat flux and water flux density on friction flow and heat transfer characteristics are examined. Experiments were performed in five cases using air as well as air/water mist two phase flow as working coolant for range of water flux density (j = 23.39 - 111.68 kg m-2 hr-1). The results obtained from the related experimental work revealed that the presence of water mist leads to a significant increase in heat transfer over the use of air coolant alone. The Nusselt numbers are respectively 1%, 19.7%, 90.2% and 134% higher than those in single phase - cooling for all cases of water flux density respectively. It was also found that the water flux density has little influence on friction factor. When the surface heat flux is fixed, the heat transfer enhancement factor increases with the increasing of water flux density.

1. Introduction

Heat transfer enhancement of a spherical heated surface or objects that are shaped as spheres is a problem of importance in a set of industrial applications such as chemical process industries and gas-cooled equipments [1]. To solve this problem, many researchers are attempting to find more effective techniques to improve the heat transfer efficiency [2]. One of the new and potentially advantageous of heat transfer enhancement techniques is air/water mist two phase flow [3]. The main features of air/water mist compared to single phase air flow can be outlined as follows: absorbs a large amount of energy in the form of latent heat during the evaporation process of water mist, increase specific heat of mixture, increase the turbulence into the air main flow and inside the boundary layer. [4]. While single-phase heat transfer and aerodynamic phenomena in spherical element has been widely studied, few studies have been found on air/water mist two phase flow. Most studies are found deal with other topics of heat transfer such as flat plate heated wall, gas turbine systems and tubular heat exchangers, including air-fine water droplets and steam-fine water droplets [5-10]. Wang et al. [11] performed a series of experiments to investigate the cooling of hot chrome-plated stainless steel plate using water mist for different surface temperatures and mist characteristics (droplet size and droplet velocity). Also Wang and Li [4, 12, and 13] numerically studied the air/water mist film cooling with 2D and 3D cases

in gas turbine system. They found by injecting 2% and 5% water mist with 10 μm droplets diameter into the coolant, the cooling performance can be improved significantly about 50-65%. Allais I and Alvarez G [14] experimentally investigated single-phase as well as two-phase flow of heat transfer rate from packed bed using air/water mist flow. The experiments were performed in low airflow velocity, low water mass flow rate and limited ranges of temperature difference. The airflow velocity and water mass flow rate were in rang (0.35 to 1.4 m s^{-1}) and (0.7 to 1.9 g s^{-1}), respectively with 8μm water droplets diameter. It was found that the total heat flux increased with increasing airflow velocity and the thermal enhancement factor increased with increasing water mass flow rate by 2.8 times under experimental conditions. A theoretical analysis of Heat and mass transfer from/to a water-droplet for the conditions pertaining to the humid air tunnel has been carried out by Barrow and Pope [15]. They reported that the time of droplet evaporation (life time) increase rapidly with increase in droplet diameter. Kim et al. [16] performed computational analysis to investigate the evaporative cooling process using moisture of air and fine water droplets by various heat and mass transfer models. Zhao and Wang [17] presented an experimental investigation to understand the film cooling enhancement by injecting tiny water droplets along with the main coolant. They pointed that the film cooling performance was enhanced significantly by dispersing water droplets with 5 μm diameters in air coolant. They also pointed that the cooling coverage increase by air/water mist coolant compared with air coolant and more uniform surface temperature can be achieved. The present experimental study proposes a new definition of heat transfer enhancement of single sphere inside a cylindrical channel with a constant uniform heat flux using air as well as air/water mist coolant as a test fluids. The influences of the different key factors such water flux density, surface heat flux and inlet Reynolds number on friction flow and heat transfer characteristics were examined.

2. Materials and Methods

An experimental facility was designed and constructed to conduct single phase as well as two phase experiments in the department of nuclear power plants and renewable energy sources / Ural Federal University, Russia. The experimental facility is composed of an air subsystem, mist subsystem, mixing section, test object with heating element and data acquisition system, a schematic layout of the experimental set-up is showed in figure 1. The air subsystem consists of transparent Plexiglas channel, which had 50 mm diameter, 3 mm wall thickness and 940 mm total length. An electrical air vacuum blower of specification (3000RPM, 1000 W) was used with variac voltage regulator to control airflow velocity. On the same axis, a compact pitot tube with digital manometer was used to measure the mean flow velocity. The test object, a 34 mm diameter sphere, was fabricated out of copper metal inserted in flow stream and it is rear supported by textolite rod (k= 0.023 W/m °C, 4mm-diameter) which span across the Plexiglas channel. The test sphere was ohmically heated by using A.C. stainless steel electrical heater type CG- high density cartridge heater whose dimension are 8mm-diameter and 31mm-length. The maximum power of A.C cartridge heater is 100W and the input power has been measured by a voltcraft digital multimeter type APPA 109N with an accuracy (±0.06%). The input power was adjusted using variac voltage regulator so as to achieve the required surface heat flux. To enhance the thermal conductance between the test sphere and A.C cartridge heater, high thermal conductivity material was used. A schematic drawing of the test sphere heat transfer model has been shown in figure 2. To measurements the surface temperature, five calibrated thermocouples type chromel-alumel were tapped in positions which are: two thermocouples placed inside the copper sphere located in positions indicated by the numbers 1, 2 as shown in figure 2, one thermocouple placed in the flow entrance region and the last two placed in the flow outlet region. The thermocouples were inserted in drilling shallow holes (diameter 1 mm) in the sphere, and the copper surface was creased around the holes to install them in place. All thermocouples are connected to data acquisition system that consists from analog signal input module type OWEN MV110-8A with MSD200 data logger. The air/water mist coolant was obtained by blending tiny water droplets (2.73 μm) in diameter into air flow. The mist subsystem was a 1.7 MHz ultrasonic mist generator consists of a piezoelectric transducers, water tank and blower fan. This type of mist generator was chosen due to the low power consumption and a very

quiet operation comparing with other mist and evaporative generators. The water mass flow rate was measured by the mass of water passing a mist subsystem per unit time. To blend the water mist supplied from mist subsystem with a controlled amount of air, a mixing chamber was installed and used as the blender.

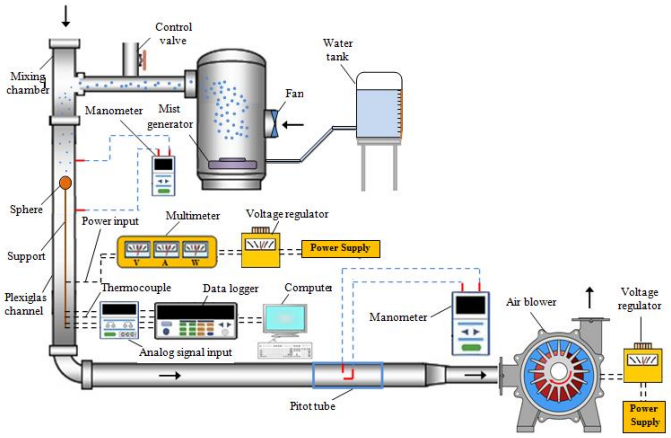

Figure 1. Schematic diagram of the experimental test bench.

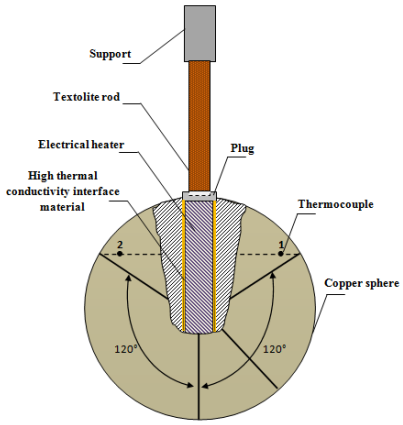

Figure 2. Schematic drawing showing the construction of heat transfer models.

In our study, The heat flux from heating system it was assumed to be uniform. It can be estimated as Eq. (1), [18].

$$q = \frac{Q_{el.} - Q_{los.}}{\mathrm{A_s}}, \tag{1}$$

where $Q_{el.}$- the input electrical power to the test sphere and $Q_{los.}$- the heat loss. The electrical power of heating system is proportional to the voltage applied to the electrical heater to maintain the required heat flux under a forced convection condition as per Eq. (2), [19].

$$Q_{el.} = \frac{V^2}{\mathrm{R}} \tag{2}$$

For a single phase flow, the average heat transfer coefficient can be described as, [20].

$$\alpha = \frac{q}{\left(T_{ave.s} - T_{ia}\right)}, \tag{3}$$

where $T_{ave.s}$ - the average surface temperature, T_{ia} - the main inlet air temperature. The water droplets trajectory can be predicted by applying Newton's second law. The energy balance equation for each droplet can be written as, [21].

$$m_p C_p \frac{dT}{dt} = \pi d^2 \alpha \left(T_{ave.s} - T_{ia}\right) + \frac{dm_p}{dt} h_{fg}, \tag{4}$$

where h_{fg} - the latent heat of evaporation. For the air/water mist flow, the average heat transfer coefficient typically can be calculated by using the wet bulb temperature at the inlet of test section as the reference temperature T_{im} that is, [21].

$$\alpha_{mist} = \frac{q}{\left(T_{ave.s} - T_{im}\right)} \tag{5}$$

$$T_{ave.s} = \sum_{x=1}^{n} \frac{T_{sx}}{n} \tag{6}$$

The water mass flow rate of mist phase is small compared to air flow. The mass flow rate is used to calculate Reynolds number as formula (7), [22].

$$\mathrm{Re} = \frac{\dot{m}\ D}{\mu A_t} \tag{7}$$

The average Nusselt number is obtained by formula (8).

$$Nu = \frac{\alpha d_s}{\lambda_a} \tag{8}$$

where d_s - the diameter of the sphere, λ_a - thermal conductivity of air. Based on the capillary wave mechanism, the droplet diameter can be calculated using Lang equation (9), [23].

$$d_p = 0.34\left(\frac{8\pi\sigma}{\rho F^2}\right)^{1/3} \tag{9}$$

where F- the working frequency of ultrasonic mist generator. The friction factor is obtained by Darcy–Weisbach equation (10), [1].

$$f = \frac{2\Delta P}{N\rho U^2} \tag{10}$$

where N - the number of sphere in channel. For a constant pumping power, the relationship between friction factor and Reynolds number can be expressed as:

$$\left(\dot{V}_a\,\Delta P_a\right) = \left(\dot{V}_m\,\Delta P_m\right) \tag{11}$$

$$\left(f\,\mathrm{Re}_a^3\right) = \left(f\,\mathrm{Re}_m^3\right) \tag{12}$$

$$\mathrm{Re}_a = \mathrm{Re}_m\left(f_m / f_a\right)^{1/3} \tag{13}$$

The thermal enhancement factor can be defined as the ratio of the heat transfer coefficient of air/water mist flow to that of a single phase flow at constant pumping power. It can be written as (14), [1].

$$\eta = \frac{\alpha_m}{\alpha_a} = \frac{Nu_m}{Nu_a} = \left(\frac{Nu_m}{Nu_a}\right)\left(\frac{f_m}{f_a}\right)^{-1/3} \tag{14}$$

The reliability of experimental facility has been presented by determining the uncertainties of experimental results [24, 25]. The uncertainty of Nusselt number can be expressed as follows:

$$\left(\frac{\Delta Nu}{Nu}\right)^2 = \frac{1}{Nu}\left[\left(\frac{\partial}{\partial \alpha}(Nu)\Delta\alpha\right)^2 + \left(\frac{\partial}{\partial d_s}(Nu)\Delta d_s\right)^2 + \left(\frac{\partial}{\partial k_s}(Nu)\Delta k_s\right)^2\right], \tag{15}$$

where $\alpha = q/(T_{ave.s} - T_{ia})$

$$\left(\frac{\Delta\alpha}{\alpha}\right)^2 = \frac{1}{\alpha}\left[\left(\frac{\partial}{\partial q}(\alpha)\Delta q\right)^2 + \left(\frac{\partial}{\partial T_{ave.s}}(\alpha)\Delta T_{ave.s}\right)^2 + \left(\frac{\partial}{\partial T_{ia}}(\alpha)\Delta T_{ia}\right)^2\right] \tag{16}$$

The uncertainties of Reynolds number and friction factor can be determined as follows:

$$\left(\frac{\Delta \mathrm{Re}}{\mathrm{Re}}\right)^2 = \frac{1}{\mathrm{Re}}\left[\left(\frac{\partial}{\partial u}(\mathrm{Re})\Delta u\right)^2 + \left(\frac{\partial}{\partial \rho}(\mathrm{Re})\Delta\rho\right)^2 + \left(\frac{\partial}{\partial D}(\mathrm{Re})\Delta D\right)^2 + \left(\frac{\partial}{\partial \mu}(\mathrm{Re})\Delta\mu\right)^2\right] \tag{17}$$

$$\left(\frac{\Delta f}{f}\right)^2 = \frac{1}{f}\left[\left(\frac{\partial}{\partial \Delta P}(f)\Delta(\Delta P)\right)^2 + \left(\frac{\partial}{\partial \rho}(f)\Delta\rho\right)^2 + \left(\frac{\partial}{\partial \mathrm{Re}}(f)\Delta \mathrm{Re}\right)^2\right] \tag{18}$$

The uncertainties of non-dimensional parameters were found to be 4%, 1.91% and 1.8%, for Nusselt number, Reynolds number and friction factor respectively.

3. Results and discussion

3.1. Effect of surface temperature

The surface temperature is an important factor that has a great influence on air/water mist heat transfer process. When the surface temperature is very hot, the water mist may be completely evaporated before arriving to the heated surface due to the force of evaporation. On the other hand, at low surface temperature, the water mist may be wet the heated surface and form a liquid film. In this study, several heat fluxes were performed to examine the effect of surface temperature on heat transfer characteristic. Figure 3, shows the average surface temperature under different heat fluxes, Reynolds number and water flux density. It can be seen that the surface temperature in single-phase flow tends to decrease gradually with raising the Reynolds number.

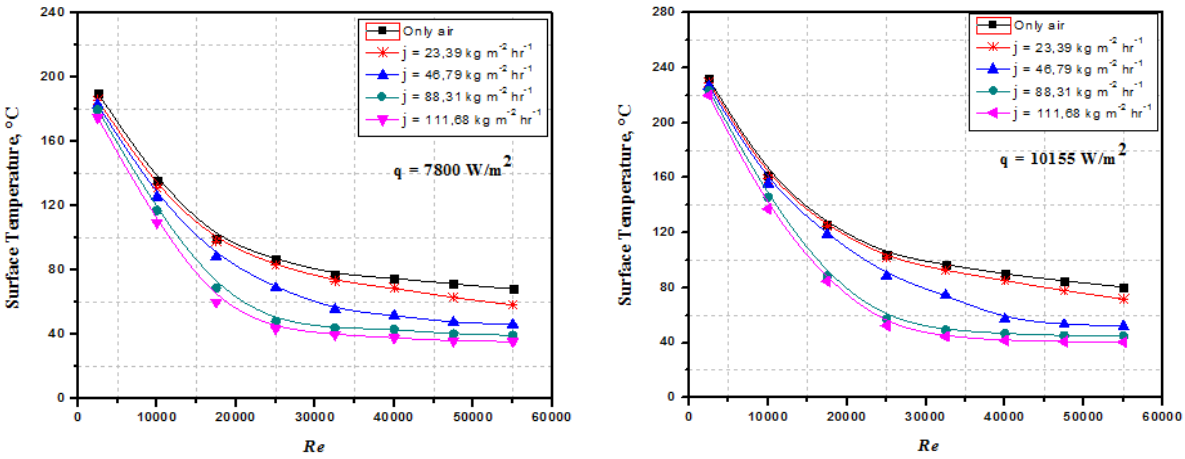

Figure 3. Variations of surface temperature of sphere with Re number under various water flux density.

In air/water mist flow, the influence of water mist evaporation appears and can be observed that the surface temperature decreases as water flux density increases for constant heat flux. The surface temperature decreases about 4%, 17%, 37% and 47% compared with air - cooling under different water flux. By the direct observation method through transparent Plexiglas channel it is observed that the heated surface covered with thin water film at high water flux density and Reynolds number (Re>17500). While the heated surface remains dry even at the lowest heat flux (q = 7800 W /m2) and Reynolds number (Re<17500), which has a surface temperature Ts > 100 °C.

3.2. Effects of Reynolds number and water flux density

The variation of average Nusselt number with Reynolds number under different water flux density is presented in Figure 4 for all cases of heat flux. In this Figures it can be observed that the average Nusselt number significantly increases as the Reynolds number increases under constant water flux density. In single-phase flow, the Nusselt number increases from 66 to 240 at range of Re number (Re = 2500 – 55000) under constant heat flux (q = 10155 W/m^2). For the Reynolds number range considered, the Nusselt numbers of air/water mist flow are respectively 1%, 19.7%, 90.2% and 134% higher than those in the single phase for range of water flux density (j = 23.39 – 111.68 kg m^{-2} hr^{-1}). In current study high Reynolds number means high main flow velocity, which drives more and more of water mist to arrive the heat transfer surface and absorbs a large amount of energy in the form of latent heat during the evaporation process. Besides, the water mist can penetrate the film-layer and enhances the heat transfer process by increasing the surface contact with main flow. As the surface temperature increases (Re<17500) the Nusselt number decrease due to water mist vaporization without wetting the heated surface. The heat transfer enhancement of air/water mist may include four important different parts: the water mist evaporation on the heating surface, sensible heat of impinging water mist, convective heat transfer based on a decline temperature gradient due to water mist evaporation in the air flow near the heated surface and enthalpy transport based on water mist departure which is effectively used for cooling. Under the conditions of q = 7800 and 10155 W/m^2 at different range of Reynolds number the average Nusselt number monotonically increases by increases the water flux density. Also it is important to mention that the maximum enhancement frequently occurs at high water concentration and low temperature surface of sphere.

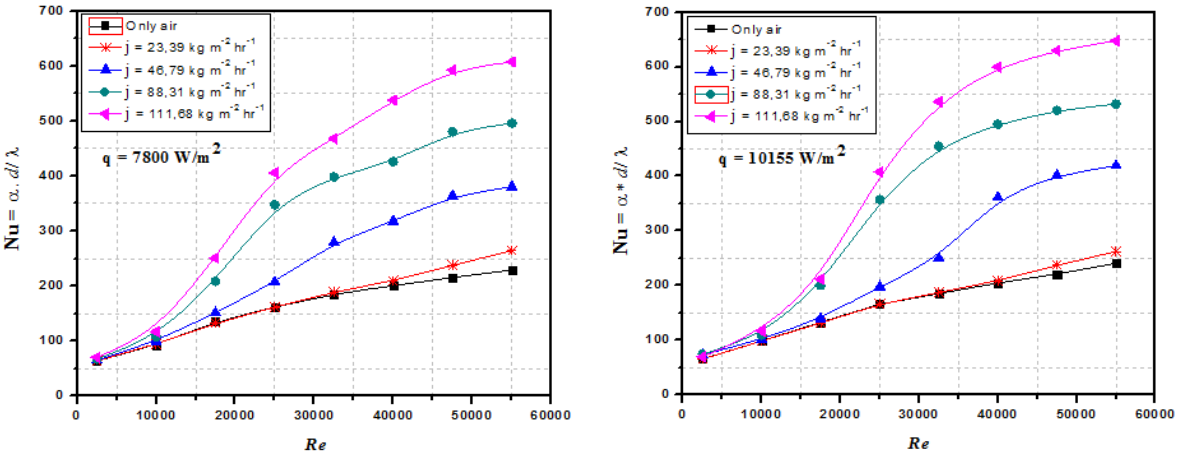

Figure 4. Variations of average Nusselt number with Re number under various water flux density.

Under range of water flux density, j = 23.39 - 46.79 kg/(m^{2}hr), with Re = 47500, the averaged Nusselt number tends to decrease with increasing of heat flux due to the low water content in the air/water mist flow, as is shown in figure 5. As water flux density increases the Nusselt number increase under range of heat flux 7800 to 10155 W/m^2. The maximum change in average Nusselt number is 8 %. The effect of using air/water mist flow on the pressure drop in the terms of friction factor with Reynolds number for all cases of water flux density are summarized in figure 6. Evidently, the friction factor decreases with the increasing of Reynolds number. Under same conditions, the friction factors that generated by air/water mist flow was little more than those generated by single phase - air coolant about 1.8 %, 3.1% 4.9% and 5.9% respectively for all cases of water flux density.

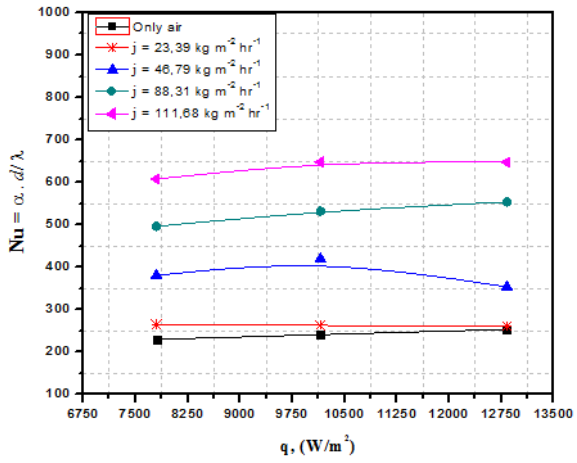

Figure 5. Variations of average Nusselt number with surface heat flux under Re = 47500 and range of water flux density

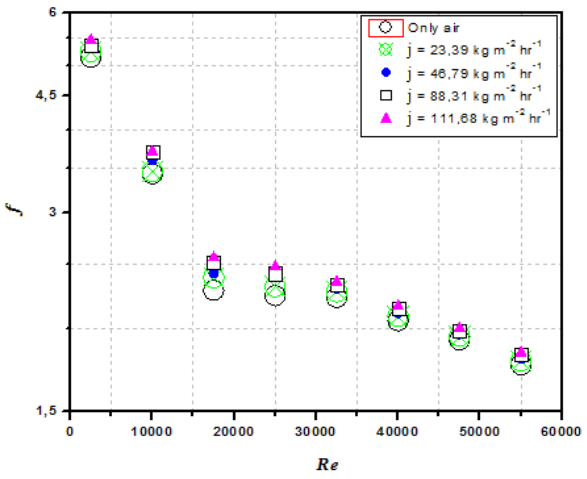

Figure 6. Variations of friction factor with Re number under different of water flux density

3.3. Thermal Enhancement Factor

Figure 7 represents the dimensionless thermal enhancement factor with Reynolds number under range of water flux density. It can be obviously seen that the thermal enhancement factor for all cases are generally more than unity and that indicate the influence of dispersing water mist into main flow on heat transfer process. At range of Reynolds number (Re = 2500 - 10000), the thermal enhancement factor were in a range between 1.0 - 1.26 for all water flux cases. This can be expressed that when the

surface temperature is very hot, the water mist may be completely evaporated before arriving to the heated surface due to the force of evaporation without wetting the heated surface.

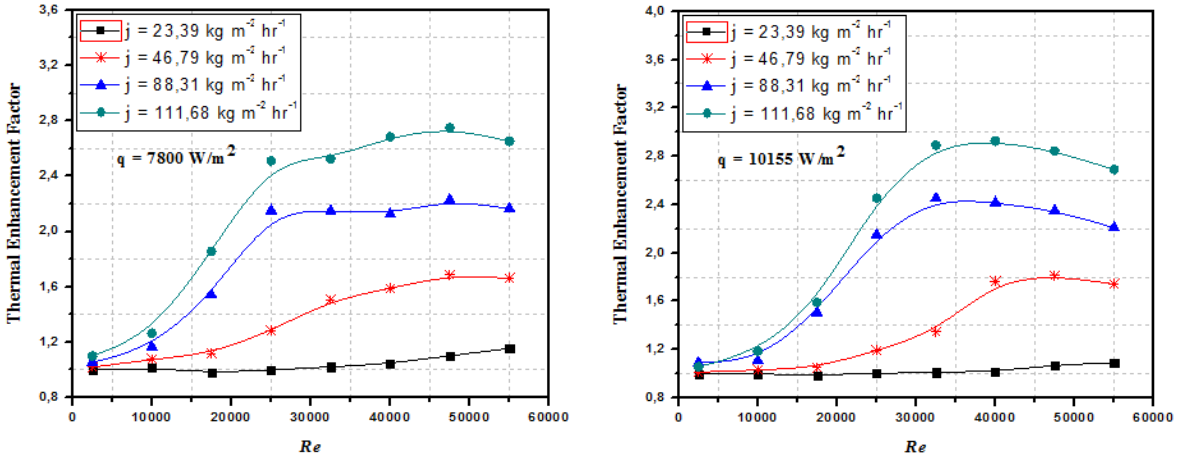

Figure 7. Variations of thermal enhancement factor with Reynolds number under range of water flux density.

The thermal enhancement factor rapidly increases with increasing of Reynolds number values (Re >17500) for all cases. At Reynolds number (Re = 40000), enhancement factor is 3 times of that with only air cooling for water flux density (111.68 kg m^{-2} hr^{-1}) under constant heat flux (q = 10155 W/m^2). The above experimental data indicates that the presence of water mist with different water concentration given more efficient heat transfer enhancement than the application of single phase - air cooling.

4. Conclusions

An open loop - cooling system using air as well as air/water mist two phase coolants was set up. The heat transfer and flow friction characteristics of a single sphere were experimentally studied in this paper. The effect of different key factors such as surface heat flux, Reynolds number and water flux density were examined. Based on the experimental results, the main conclusions can be summarized as follows:

- The air/water mist cooling technique is a very efficient way to remove a great deal of heat from sphere surface. The surface temperature decreases about 4%, 17%, 37% and 47% compared with air - coolant by using different water flux density.
- The average Nusselt number significantly increases as the Reynolds number increases under constant heat flux and water flux density. By using water mist, the average Nusselt numbers are respectively 11%, 19.7%, 90.2% and 134% higher than those in the air - coolant for water flux density (j=23.39 to 111.68 kg m^{-2} hr^{-1}). The average Nusselt number is slowly increased with increasing heat flux when the water flux density and Reynolds number are fixed.
- The friction factor is generally decreases with the increasing of Reynolds number. Under same conditions, the friction factors that generated by air/water mist coolant was little more than those generated by air - coolant about 1.8 %, 3.1%, 4.9% and 5.9% respectively for all cases of water flux density.
- The enhancement factors for all cases are generally more than unity indicating that the presence of water mist with different water concentration given more efficient heat transfer enhancement than the application of single phase - air cooling.

Acknowledgments
The work was supported by Act 211 Government of the Russian Federation, contract № 02.A03.21.0006

References
[1] Jiang G, Shi X, Chen G and Gao J 2018 *Int. J. Heat Mass Transf.* **120** 1101-17
[2] Xishi W, Guangxuan L, Weicheng F and Dobashi R 2004 *J. Fire Sci.* **22(5)** 355-66
[3] Zhao L and Wang T 2014 *J. Turbomach.* **136(7)** 071007
[4] Wang T and Dhanasekaran T 2010 *J. Heat Transf.* **132(12)** 122201
[5] Yang W J and Clark D W 1975 *Int. J. Heat Mass Transf*.**18** 311317
[6] Nakayama W, Kuwahara N and Hirasawa S 1988 *Int. J. Heat Mass Transf*. **11(2)** 449-60
[7] Dreyer A, Kriel D and Erens P 1992 *Heat Transfer Engineering* **13(4)** 53-71
[8] Thomas W and Sunderland J 1970 *Ind. Eng. Chem. Fundam.* **9(3)** 368-74
[9] Hwang T 1990 *Int. J. Heat Mass Transf.* **33(5)** 943-52
[10] Hayashi Y, Takimoto A, Matsuda O and Kitagawa T 1990 JSME international journal. Ser. 2, Fluids engineering, heat transfer, power, combustion, thermophysical properties 33(2) 333-39
[11] X S Wang, G X Liao and W C Fan 2004 *J. Fire Sci.* **22** 355–66
[12] X Li and T Wang 2006 *J. Heat Transf.* **128** 509–19
[13] X Li and T Wang 2007 *J. Heat Transf.* **129** 472–82
[14] Allais I and Alvarez G 2001 *Journal of Food Engineering* **49(1)** 37-47
[15] Barrow H and Pope C 2007 *Applied Energy* **84(4)** 404-12
[16] Kim K, Ko H, Kim K and Perez-Blanco H 2012 *Appl. Therm. Eng.* **33-34** 62-69
[17] Zhao L and Wang T 2014 *J. Turbomach.* **136(7)** 071006
[18] Quinn C, Murray D and Persoons T 2017 *Int. J. Heat Mass Transf*. **111** 1234-49
[19] Yoon S and NO H 2017 *Nuclear Engineering and Design* **325** 97-106
[20] Tao Y, Huai X, Wang L and Guo Z 2011 *Appl. Therm. Eng.* **31(10)** 1790-97
[21] Li X and Wang T 2008 *J. Heat Transf.* **130(10)** 102901
[22] Abed A and Shcheklein S 2018 *J. Phys.: Conf. Series* **1015** 032001
[23] R J Lang 1962 *J. Acoust. Soc. Am.* **34** 6–8
[24] S J Kline and F A McClintock 1953 *Mechanical Engineering* **75** 3–8
[25] Kline S J 1953 *Mech. Engineering* **75** 3-8